THE QUANTITATION OF NUCLEAR OVERHAUSER EFFECT METHODS FOR TOTAL CONFORMATIONAL ANALYSIS OF PEPTIDES IN SOLUTION

APPLICATION TO GRAMICIDIN S

CLAUDE R. JONES, CYNTHIA T. SIKAKANA, SEAN HEHIR, MEI-CHANG
KUO, AND WILLIAM A. GIBBONS, *Department of Biochemistry,*
College of Agricultural and Life Sciences, University of Wisconsin-Madison,
Madison, Wisconsin 53706 U.S.A.

ABSTRACT   The [^{1}H:^{1}H] nuclear Overhauser effects (NOE's) and spin-lattice relaxation times (T_1's) are reported for the backbone protons of the decapeptide gramicidin S. Several methods for calculating interproton distances from these measurements are presented.   Ratios of interproton distances were obtained from [^{1}H:^{1}H] NOE's and from the combination of [^{1}H:^{1}H] NOE's and T_1 values. Actual proton-proton distances were calculated from these ratios either by using the known distance between two geminal protons or distances derived from scalar coupling constants. The interproton distances calculated for gramicidin S are consistent with a II' β-turn/ antiparallel β-sheet conformation.

INTRODUCTION

Double irradiation and the selective changes in the intensities of nuclear magnetic resonance (NMR) lines it produces form the basis of the two valuable NMR techniques (1, 2), internuclear double resonance (INDOR) and nuclear Overhauser effect (NOE). INDOR has been used to simplify spectra, to reveal hidden transitions, and to study the stereochemistry of amino acids and peptides by providing a measure of through-bond interactions (scalar coupling) (3, 4). NOE has been used to measure through-space interactions (dipolar coupling) and consequently it has provided a complimentary method of studying amino acid and peptide conformation (5–10). Overhauser effects that arise from the transfer of saturation by chemical exchange have also been useful, particularly in studies of protein-peptide interactions (11) and peptide-solvent interactions (12, 13). These results indicate that an accurate, total conformation analysis of a complex peptide such as the decapeptide gramicidin S might now be possible.

Gramicidin S has been the object of numerous NMR (4, 6, 8, 10, 13–28) and theoretical studies (18, 29–42), but much remains to be elucidated.   A β-pleated sheet–β-
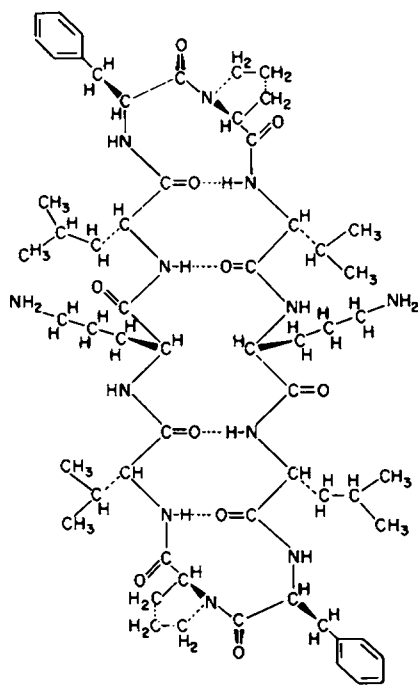
FIGURE 1   The structure of gramicidin S, cyclo-(pro-val-orn-leu-D-phe)₂.

turn model for the conformation of gramicidin S was indicated by scalar coupling constant measurements ($^3J_{NHCH}$) (15, 18) and NMR hydrogen-bonding criteria (8, 13, 14, 8, 22, 23) (Fig. 1). It has also been established by ^{13}C NMR (21, 24), that the backbone atoms have the same correlation time and that extensive rotation of the side-chains occurs. Difference double resonance studies (35–37) gave the statistical weights of the χ_1 side-chain rotamers as well as the statistical weights of tertiary conformations of the whole molecule. Significantly absent from these experimental results were accurate determinations of the dihedral angles, ψ, and resolution of which of the four possible ϕ angles consistent with each measured $^3J_{NHCH}$ value was correct.

Preliminary NOE studies tested specific aspects of the proposed gramicidin S model. It was shown in 1975 (6), for example, that the NOE's between peptide backbone protons were qualitatively consistent with the antiparallel β-sheet model and the NOE detected between the Phe C$^\alpha$H and Pro C$^\delta$H protons agreed with the proposed β-II' turn. Glickson et al. (8) established the dipolar nature of these NOE's, Rae et al. (10) provided partial quantitation, and Khaled and Urry (7) confirmed that NOE's could distinguish the β-turns in elastin peptides. As a result of an investigation of the conformation of gramicidin S using NOE and relaxation measurements, we are able to report: (a) that we determined NOE's between all backbone protons by NOE difference spectroscopy (NOEDS); (b) that qualitative NOE criteria (6) for β-turns, β-sheets, and regular structures in peptides can be put on a quantitative basis; (c) that gramicidin

S NOE and T_1 data are consistent with an approximate β-pleated sheet and a β-II' turn; (d) that interproton distances have been calculated by two independent methods, one using distances derived from scalar coupling constants and the other using known geminal interproton distances.

THEORY

The origins of the (^{1}H:^{1}H) NOE have been extensively investigated and a comprehensive review published (38). The large, negative NOE's observed for peptides at high magnetic field strength are known to be predominately dipole-dipole in origin (8), permitting an application of the standard numerical treatment. (38) The fractional change in intensity of a resonance, d, when the transitions of spin, s, are saturated is

$$\text{NOE}_d(s) = (<I_{zd}> - I_{od})/I_{od}, \tag{1}$$

where $<I_{zd}>$ is the average value of the z component of spin angular momentum of spin d and I_{od} is its equilibrium value. The observed NOE's are related to the relaxation parameters σ and R by:

$$\text{NOE}_d(s) = \frac{\sigma_{ds}}{R_d} - \sum_{j \neq d,s} \left[\frac{\sigma_{dj}}{R_d} \left(\frac{<I_{zj}> - I_{oj}}{I_{od}} \right) \right]. \tag{2}$$

R_d is the spin lattice relaxation rate and includes nondipole-dipole interaction terms, such as the contribution from ^{14}N quadrupolar relaxation, as well as the sum of all dipole-dipole interaction terms. R_d just equals $1/T_1^{SE}$, where T_1^{SE} is the spin lattice relaxation time measured when all other I_z are constant during the measurement; the selective excitation method (39, 40) is a convenient way to measure T_1^{SE}. The second term on the right accounts for the indirect contributions to an observed NOE that result from partial saturation of protons other than d or s.

None of the NOE's reported here have magnitudes larger than 0.183, and the partial saturations are usually small enough that the second term in Eq. 3 can be evaluated by successive approximations, where this term can be written to a first approximation,

$$\frac{\sigma_{dj}}{R_d} \left(\frac{<I_{zj}> - I_{oj}}{I_{od}} \right) = \text{NOE}_d(j) \left(\frac{<I_{zj}> - I_{oj}}{I_{od}} \right), \tag{3}$$

where the term in brackets is the fractional change in intensity of j when s is saturated. The partial saturations and $\text{NOE}_d(j)$ terms were never large enough to require interactive application of Eq. 3.

When only dipole-dipole mechanisms contribute significantly to the two quantum transitions W_0 and W_2, then (8, 38),

$$\sigma_{ds} = W_2^{ds} - W_0^{ds} = \frac{1}{r_{ds}^6} \frac{\gamma^4 \hbar^2}{10} \left[\frac{6\tau_c}{1 + 4\omega_H^2 \tau_c^2} - \tau_c \right], \tag{4}$$

where ω_H is the Larmor frequency for protons. Since

$$\sigma_{ds}/R_d = T_1^{SE}(\sigma_{ds}) \tag{5}$$

σ's could be calculated for each observed NOE when the corresponding T_1^{SE} were also measured. Allerhand and Komorski, (21) found that gramicidin S could be treated as an isotropic rotor and that τ_c was just equal to the rotational reorientation time. Consequently in the ratio of any two σ's, all the terms in Eq. 4 cancel except the $1/r^6$ terms. If one interproton distance as well as the corresponding σ's are known, any other interproton distance can be calculated from the corresponding σ. In cases where irradiation of two different protons, say s and m, both produce NOE's at proton d, then it is not necessary to measure the R_1^{SE}'s since $(\sigma_{ds}/R_d)/(\sigma_{dm}/R_d) = \sigma_{ds}/\sigma_{dm} = (1/r_{ds}^6)/(1/r_{dm}^6)$.

METHODS

Samples were prepared by dissolving 2 mg of gramicidin S (Sigma Chemical Co., St. Louis, Mo.) in 0.5 ml of dried, 100% deuterated dimethyl sulfoxide. For each spectrum 5,000–6,000 transients were accumulated at $26 \pm 1°C$ in the pulse mode with a Bruker Scientific WH 270 (Bruker Instruments, Inc., Billerica, Mass.), interfaced with a Nicolet 1180 computer (Nicolet Instrument Corp., Madison, Wis.). The free induction decays (FID's) were multiplied by an exponent before the Fourier transform was taken to produce a 1 Hz line broadening. Subtracting an off-resonance control FID from a FID produced when one proton was presaturated by a 2-s gated pulse (6) produced the NOEDS. NOE'S were measured directly from the NOEDS. In order to select a decoupling power sufficient for saturation with a 2-s pulse, the NOE's were measured as a function of power. Comparison of the integrated areas of a peak in the NOEDS with an area in the control spectrum that had a known number of contributing proton resonances gave the fractional changes an intensity of a given resonance per unit proton—the numerical values of the NOE's (Table I).

The method of selective excitations (39, 40) was used to measure the proton spin-lattice relaxation times (T_1^{SE}) was used to measure the proton spin-lattice relaxation times (T_1^{SE}) of gramicidin S. The 180°-τ-90° sequence was generated as follows: the selective 180° pulse was generated by the decoupler channel and was usually ~ 10 ms in duration with a very narrow band width, approximately 50 Hz. The 90° pulse was the usual high-power, 10-μs pulse. The T_1^{SE}'s were measured from the initial rates of decay, which appeared to be exponential.

The 270 MHz spectrum of gramicidin S in dimethyl sulfoxide (DMSO-d_6) is shown in Fig. 2. The val NH T_1^{SE} and phe C$^\alpha$H T_1^{SE} values could not be accurately measured because of extensive overlap with the nearby resonances. Although overlap of the val, phe, and pro C$^\alpha$H multiplets occurs at ~ 4.3 ppm, accurate T_1^{SE} values for val C$^\alpha$H and pro C$^\alpha$H were obtained, since individual resonances from their multiplets were still visible. Some collateral perturbations of C$^\alpha$H magnetization was necessarily produced by inversion of the val C$^\alpha$H and pro C$^\alpha$H spins but since the dipole-coupled side chain and amide protons were unaffected by the selective inversion pulse, the practical requirements of selective excitation were met, viz. each proton spin lattice relaxation time was measured while the magnetization of all of the other, dipole-coupled protons was constant. Measurement of T_1^{SE} values for all other amide protons, and for leu C$^\alpha$H and pro C$^\delta$H was straightforward.

TABLE I

AREAS OF PEAKS IN NOEDS DUE TO NOE'S AND DIRECT EFFECTS OF DECOUPLER EXPRESSED IN FRACTIONS OF ONE PROTON

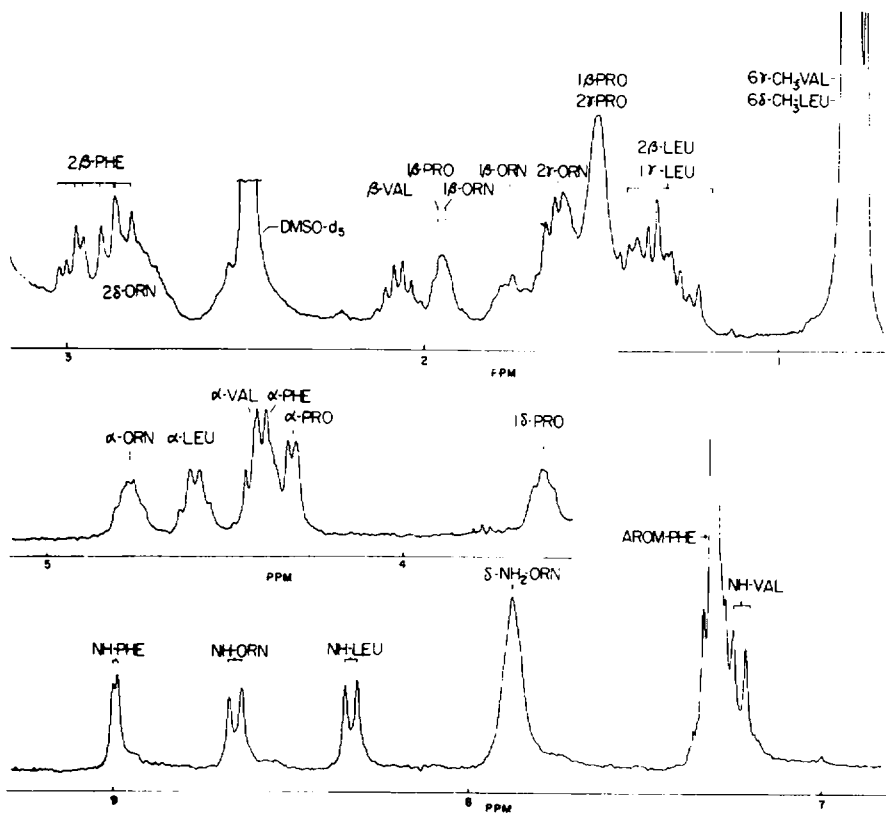| Irradiated proton	Intensity change observed at									
	(1) Orn NH	(2) Leu NH	(3) Phe NH	(4) Val C$^\alpha$H	(5) Orn C$^\alpha$H	(6) Leu C$^\alpha$H	(7) Phe C$^\alpha$H	(8) Pro C$^\alpha$H	(9) Pro C$^\delta$H1	(10) Pro C$^\delta$H2
Val NH	—	—	—	-0.029	—	—	-0.029	-0.059	—	—
Orn NH	-1	-0.035	-0.031	-0.170	-0.027	-0.008	—	—	—	—
Leu NH	-0.037	-1	-0.024	—	-0.129	-0.025	—	—	—	—
Phe NH	-0.035	-0.019	-1	—	—	-0.126	-0.027	—	—	—
Val C$^\alpha$H	-0.081	—	-0.024	-1	-0.031	-0.116	-0.830	-0.560	—	—
Orn C$^\alpha$H	-0.019	-0.082	-0.022	-0.040	-1	-0.280	-0.040	-0.040	—	—
Leu C$^\alpha$H	-0.029	-0.026	-0.079	-0.230	-0.136	-1	-0.230	-0.120	—	—
Phe C$^\alpha$H	-0.079	-0.007	-0.023	-0.800	-0.020	-0.081	-1	-0.600	-0.078	-0.070
Pro C$^\alpha$H	-0.047	—	-0.022	-0.420	-0.021	-0.047	-0.580	-1	—	—
Pro C$^\delta$H1	-0.011	-0.011	-0.014	—	—	—	-0.100	—	-1	-0.183
Pro C$^\delta$H2	-0.007	—	-0.016	—	—	—	-0.117	—	-0.163	-1

FIGURE 2 The 270 MHz NMR spectrum of gramicidin S in DMSO-D$_6$ with assignments made by NOEDS (37).

RESULTS

NOEDS

A typical NOE experiment, such as the one shown in Fig. 3, consists of a control spectrum, a spectrum obtained when one resonance is saturated, and the difference between the two. There are several advantages in measuring NOE's from these double resonance difference spectra rather than direct measurements of intensities in experimental and control spectra. First, significant NOE's are readily apparent in the NOEDS; it is not necessary to measure every single peak to be sure that all significant NOE's have been observed. Second, resonances from protons unaffected by the saturating pulse cancel, allowing NOE's to be measured even when a resonance is not totally resolved from all other resonances. Third, computer substraction, followed by measurement of small deviations of integrated intensity from zero, is much more accurate than measurement of two large and only slightly different areas followed by subtraction.

In the NOEDS in Fig. 2 a number of peaks appear in the NH region, the largest due
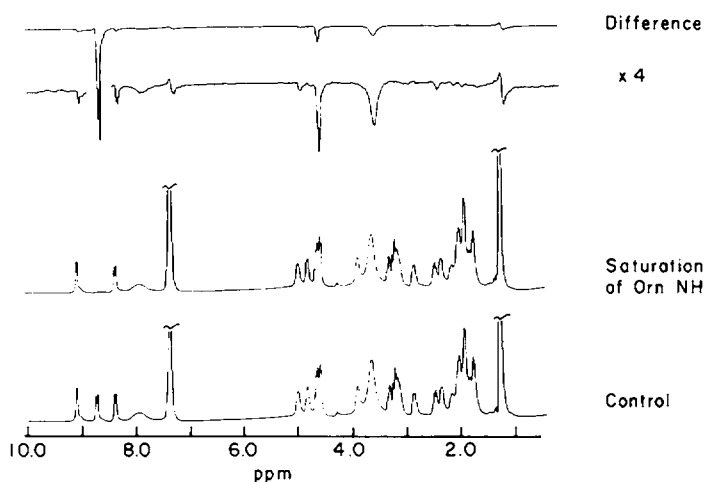
FIGURE 3 (*top*) The control spectrum obtained with the decoupler frequency set to a value at which no resonances occurs; (*middle*) the spectrum obtained when the decoupler was set to saturate the transitions of the orn NH; and (*bottom*) the NOEDS obtained by subtracting the second from the first. The NOEDS shows two NOE's in the $C^{\alpha}H$ region (4.5–5.5 ppm), the most prominent of which is the NOE at the val $C^{\alpha}H$.

to the orn NH resonance exactly at the decoupler frequency. Signals of intensity −0.03 proton are seen on both sides of the orn NH peak, one on the high field side, the phe NH, and one on the low field side, the leu NH. Both are accounted for by direct, partial saturation by the decoupler (decoupler spillover). While these partial saturations do not correspond to significant σ/R_d terms themselves, they must be corrected for (Eqs. 2 and 3) in the calculation of σ/R_d terms from authentic NOE's. In the case of the NOE's in Table I the iterative application of Eq. 4 never needed to be carried to two steps to make this correction, even in the instances of largest spillover.

In the $C^{\alpha}H$ region of Fig. 2, 4–5 ppm, the most prominant feature is the −17% intensity change at the val $C^{\alpha}H$. It is quite clear that there are two other NOE's in the $C^{\alpha}H$ region of the NOEDS in Fig. 2. The smaller one (−0.008) at the leu $C^{\alpha}H$ is due mainly to the partial saturation of the phe NH. Taking the partial saturation into account (Table II) leaves a calculated σ/R_d of only −0.003, experimentally insignificant. The second of the small NOE's in the $C^{\alpha}H$ region, the fractional change of 0.027 at the orn $C^{\alpha}H$ resonance, has two contributions. A minor part is due to the partial saturation of the leu NH; by using Eq. 3 this contribution is calculated to be 19% of the observed NOE and the rest is due to the orn NH–orn $C^{\alpha}H$ dipolar interaction. The ability to measure four of these intraresidue terms is quite valuable, since they are directly related to the dihedral angle ϕ and an independent measurement of ϕ angles is available for $^3J_{\text{NHCH}}$ values.

Some other signals in the NOEDS can also be seen. The residual water in the NMR sample gives a very broad peak at 3.3 ppm in the DRD spectrum. We attribute this to saturation transfer by chemical exchange of the orn NH rather than a dipole-

TABLE II
VALUES OF σ_{ds}/R_d CALCULATED FROM THE DATA IN TABLE I (EQ. 3)

Proton saturated (s)	Proton observed (d)									
	Orn NH	Leu NH	Phe NH	Val C^αH	Orn C^αH	Leu C^αH	Phe C^αH	Pro C^αH	Pro C^δH1	Pro C^δH2
Val NH				(d) −0.029						
Orn NH				(a) −0.170	(e) −0.022	−0.003		−0.054		
Leu NH				−0.006	(b) −0.128	(f) −0.022				
Phe NH						(c) −0.126	(g) −0.027			
Val C^αH	(a) −0.081		−0.002							
Orn C^αH	(e) −0.016	(b) −0.082								
Leu C^αH	(h) −0.010	(f) −0.015	(c) −0.079							
Phe C^αH	(i) −0.014	−0.004	(g) −0.017							
Pro C^αH			−0.01							
Pro C^δH1							−0.081		−0.067	−0.056
Pro C^δH2							−0.104		−0.154	−0.177

(a)–(i) Values with the same superscript are for the same dipole-dipole interaction.

dipole coupling mechanism; the reverse saturation transfer is well-known in peptides if the NH is not protected from solvent (13). In the phe aromatic proton region (7.3 ppm) and methyl region (0.9 ppm) peaks with regions of both positive and negative intensity are observed. The shapes indicate that the peaks are largely due to subtraction errors, which could be as large as 0.5% of a proton in the positive direction or 0.5% of a proton in the negative direction. Consequently, ±0.005 proton is taken to be the accuracy of subtraction of two spectra. This is to be added to the ±0.018 (10%) and ±0.002 (16%) proton uncertainties in measuring the areas of the largest and smallest NOE's, respectively.

Calculation of σ/R_d Values

Values of σ/R_d were calculated from Eq. 2 with the estimates of the effects of cross-polarization and decoupler spillover given by Eq. 3. These values could have been used to calculate the cross-polarization effects to a higher approximation than that given by Eq. 3, but since the cross-polarization effects were generally small, a second iterative cycle of cross-polarization corrections was not needed. This is a fortunate case; the NOE's are negative and large enough to be accurately measured but not so large that extensive corrections for cross-polarization are important. Furthermore, there was enough resolution to evaluate both the effects of backbone-backbone and backbone-side chain NOE's. The σ/R_d values in the upper middle of Table II were obtained from experiments when each NH was irradiated and the $C^\alpha H$'s were observed, while the σ/R_d terms in the lower left were obtained when each $C^\alpha H$ was irradiated and the NH's were observed. The σ/R_d values a-c are notably larger than all of the others in both cases. These are nearest-neighbor interresidue $C^\alpha H \leftrightarrow NH$ effects and their size shows that the corresponding protons are very close to each other. All four intraresidue $NH \leftrightarrow C^\alpha H$ σ/R_d terms, d-g were also observed. The intraresidue σ/R_d values obtained when the $C^\alpha H$'s were observed and the NH's were saturated (top middle of Table II) are more accurate than those obtained when the $C^\alpha H$'s were saturated and the NH's observed. In the latter case the corrections for decoupler spillover were larger, due to the close spacing of the val, phe, pro group of C^α resonances, and required computer simulation of $C^\alpha H$ region of the NOEDS.

Calculation of σ's

The spin-lattice relaxation times measured by selective excitation, T_1^{SE} (Table III), contribute considerably to the understanding and use of the NOE data. Values of σ can be calculated for many of the dipolar interactions among backbone protons (Eq. 5), and these are given in Table IV. In cases where there are two entries, the values were calculated from different NOE's and different T_1^{SE}'s. Consequently the comparison of the two values can test the accuracy and internal consistency of the T_1^{SE}-NOE data. The two σ(phe NH-leu $C^\alpha H$) values for example, one calculated from NOE_{pheNH}(leu $C^\alpha H$) and one calculated from $NOE_{leu\ C^\alpha H}$(phe NH) only differ by 12%. These NOE's are quite different, -0.079 and -0.126, respectively, but the difference is entirely contained in the $1/T_1^{SE}$ term. Thus NOE's observed either at the

Residue	Proton			
	NH	$C^\alpha H$	$C^\delta H1$	$C^\delta H2$
		ms		
Val		458		
Orn	223			
Leu	250	370		
Phe	261			
Pro		682	205	227

	Orn NH	Leu NH	Phe NH	Val NH	Pro C^δHI	Pro C^δH2
Val $C^\alpha H$	−0.363 −0.371			−0.063		
Orn $C^\alpha H$	−0.072	−0.328				
Leu $C^\alpha H$		−0.060 −0.059	−0.303 −0.341			
Phe $C^\alpha H$			−0.064		−0.327	−0.247
Pro $C^\alpha H$				−0.087		
Pro C^δH1						−0.751 −0.780

$C^\alpha H$ or at the NH protons are equally useful measurements of the NH—$C^\alpha H$ dipolar interaction.

DISCUSSION

The values of NOE's between backbone protons give considerable insight into peptide structure; relatively large values indicate that the corresponding protons are close together and vice versa for small values. For gramicidin S the alternating pattern of large nearest-neighbor interresidue NOE's and small intraresidue NOE's is exactly the pattern predicted from the β-turn/β-pleated sheet model. However, it is possible to go beyond qualitative use of this data and obtain some quantitative estimates of the distances between backbone protons. Four different methods of calculating backbone interproton distances were used; two different ways of calculating the ratios of interproton distances and with each two different ways of obtaining a single known, "calibration" distance.

Method I: NOE Measurements and Geminal Interproton Distances

In gramicidin S the two pro C^δH's have much different chemical shifts so the NOE's involving each of them could be obtained separately. Furthermore, the distance be-

TABLE V

CALCULATED INTERPROTON DISTANCES BASED ON r(PRO C^δH1 – PRO C^δH2) AND σ_{ds}/R_d VALUES IN TABLE II

Distance	Å
r(pro C^δH1—pro C^δH2)	1.77
r(phe C^αH—pro C^δH2)	2.03
r(phe C^αH—pro C^δH2)	2.14
r(phe NH—phe C^αH)	2.43
	2.68
r(phe NH—leu C^αH)	1.88
	2.07
r(leu NH—leu C^αH)	2.33
	2.56
r(leu NH—orn C^αH)	1.75
	1.93
r(orn NH—orn C^αH)	2.35
	2.59
r(orn NH—val C^αH)	1.79
	1.98
r(val NH—val C^αH)	2.40
	2.66

tween these geminal protons can be calculated from standard bond lengths and bond angles (41). With this distance known and the σ_{ds}/R_d values in Table II, the length of each interproton distance for the gramicidin S backbone was calculated using Eq. 6 (Table V). The "observed" proton must be the same for both NOE's in Eq. 6, so strings of these ratios were combined to relate the r(pro C^δH1—pro C^δH2) to interproton distances further and further along in the sequence.

Method II: NOE Measurements and Interproton Distances from $^3J_{NHCH}$ Values

This method is also based on $\sigma's/R_d$ values but takes the intraresidue H—C^α—N—H interproton distances obtained from measured $^3J_{NHCH}$ values as the known distances. The results calculated from this method are given in Table VI. For each $^3J_{NHCH}$ value the Karplus-Bystrov curve (42) was used to calculate the ϕ angles; standard bond lengths and bond angles (41) were assumed to calculate the H—C^α—N—H distance. In general four possible ϕ angles and therefore four possible H—C^α—N—H distances are consistent with a given $^3J_{NHCH}$ value. However, for the val, orn, and leu residues the coupling constants were so large that only two possible ϕ angles and two possible distances were obtained for each, and furthermore, within the accuracy of coupling constant measurements, the two values were equal for each of these residues. For the D-phe residue there were essentially two distinct possible H—C^α—N—H interproton distances, 2.37 and 2.84 Å, but only one of these, 2.84 Å, gave distances consistent with the results based on the other coupling constants. In Table VII the distances marked § were determined directly from the $^3J_{NHCH}$ values; the rest of the

TABLE VI

INTERPROTON DISTANCES CALCULATED FROM THE RATIOS IN
TABLE V AND VICINAL COUPLING CONSTANT DISTANCES

Distances	Coupling constants and possible ϕ angles				Mean	SD
	$^3J_{\text{NHCH}}(\text{phe})$ $=4.41$ Hz* $(-105°)\ddagger$ $(-14°)$ $(+173°)$ $(+67°)$	$^3J_{\text{NHCH}}(\text{leu})$ $=9.94$ Hz* $(-138°)\ddagger$ $(-103°)$	$^3J_{\text{NHCH}}(\text{orn})$ $=10.42$ Hz* $(-132°)\ddagger$ $(-108°)$	$^3J_{\text{NHCH}}(\text{val})$ $=10.22$ Hz* $(-135°)\ddagger$ $(-106°)$		
			$\overset{\circ}{A}$			
$r(\text{pro C}^\delta\text{H1—pro C}^\delta\text{H2})$	2.08	2.24	2.22	2.16	2.07	0.13
	1.87	2.03	2.01	1.97		
$r(\text{phe C}^\alpha\text{H—pro C}^\delta\text{H1})$	1.92	2.08	2.06	2.02		
	2.39	2.57	2.55	2.49	2.50	0.08
$r(\text{phe C}^\alpha\text{H—pro C}^\delta\text{H2})$	2.27	2.46	2.44	2.39	2.39	0.09
$r(\text{phe NH—phe C}^\alpha\text{H})$	2.84§	3.08	3.06	2.99	2.99	0.11
$r(\text{phe NH—leu C}^\alpha\text{H})$	2.20	2.38	2.37	2.31	2.31	0.08
$r(\text{leu NH—leu C}^\alpha\text{H})$	2.72	2.95§	2.93	2.86	2.87	0.10
$r(\text{leu NH—orn C}^\alpha\text{H})$	2.05	2.22	2.21	2.16	2.16	0.08
$r(\text{orn NH—orn C}^\alpha\text{H})$	2.75	2.98	2.96§	2.89	2.90	0.10
$r(\text{orn NH—val C}^\alpha\text{H})$	2.10	2.27	2.26	2.20	2.21	0.08
$r(\text{val NH—val C}^\alpha\text{H})$	2.81	3.05	3.03	2.96§	2.96	0.11

*Measured values of the coupling constants[37] after electronegativity corrections have been made[42].
‡Possible values of ϕ calculated from the Karplus-Bystrov relation[42].
§Distances calculated directly from ϕ and used to calculate the other distances in the column.

distances in the same column were calculated using this known distance as a "calibration."

Method III: Combined Use of NOE, T$_1^{SE}$ Measurements, and Geminal Proton Distances

In this method (Table VII) the $r(\text{pro C}\delta\text{H1—pro C}\delta\text{H2})$ distance was used for "calibration" but instead of ratios of σ_{ds}/R_d, ratios of σ_{ds} values were used to calculate ratios of distances with Eq. 6. In this case the observed proton does not have to be common to the two measurements to get a ratio of distances from a single ratio of experimentally measured parameters. The ratio between $r(\text{pro C}\delta\text{H1—pro C}\delta\text{H2})$ and any other interproton distance can be determined provided the corresponding σ has been measured.

Method IV: Combined Use of NOE and T$_1^{SE}$ Measurements and Interproton Distances from $^3\text{J}_{NHCH}$ Values

This method again uses distance ratios calculated from σ_{ds}'s for calibrations, uses interproton H—C$^\alpha$—N—H distances calculated from $^3J_{\text{NHCH}}$ values. It is interesting to note that, for example, the $r(\text{leu NH—leu C}^\alpha\text{H})$ distance in Table VIII was obtained from calculations based on $^3J_{\text{NHCH}}$ (phe), $^3J_{\text{NHCH}}$ (leu), $^3J_{\text{NHCH}}$ (orn), and $^3J_{\text{NHCH}}$ (val) and the four values are in excellent agreement; the standard deviation

TABLE VII

Distance calculated	Distance	Average	SD
	$\overset{\circ}{A}$		
r(pro C^δH1—pro C^δH2)	1.77*		
r(pro C^δH1—phe C^αH)	2.03	2.04	0.01
	2.05		
r(pro C^δH2—phe C^αH)	2.13	2.14	0.01
	2.14		
r(phe NH—phe C^αH)	2.68	2.73	0.01
	2.68		
r(phe NH—leu C^αH)	2.06	2.05	0.02
	2.02		
	2.07		
	2.03		
r(leu NH—leu C^αH)	2.70	2.71	0.01
	2.70		
	2.71		
	2.72		
r(leu NH—orn C^αH)	2.03	2.04	0.01
	2.04		
r(orn NH—orn C^αH)	2.62	2.63	0.01
	2.63		
r(orn NH—val C^αH)	2.00	2.00	0.01
	1.99		
	2.01		
	2.00		
r(val NH—pro C^αH)	2.53	2.54	0.01
	2.55		
r(val NH—val C^αH)	2.68	2.69	0.01
	2.69		

*This geminal distance obtained from standard bend lengths and bond angles[41] was used in the calculation of all other distances.

is 0.11 Å. Averaging the four r(leu NH | leu C^αH) values averages the individual $^3J_{\text{NHCH}}$, NOE, and T_1^{SE} measurements but does not remove any systematic errors involved in the calibration of the Karplus-Bystrov curve.

The accuracy of calculated distances can be estimated since the expected error in an interproton distance r_1 calculated from Eq. 6 is $\lambda(r_1) = \{[r_2^{-1}r_1]^2\lambda^2(r_2) + [\frac{1}{6}(\sigma_{12}/R_2)^{-1}r_1]^2\lambda^2(\sigma_{12}/R_2) + [-\frac{1}{6}(\sigma_{12}/R_1)^{-1}r_1]^2\lambda^2(\sigma_{12}/R_1)\}^{1/2}$. For the case of $r_1 = r$(orn NH—val C^α H) (Table VI, column 4), $\lambda(r_1) = [0.59(0.17)^2 + 213(0.008)^2 + 6.3(0.022)^2]^{1/2} = 0.17$ Å. Where the uncertainty in the NOE measurements λ(NOE) is given in the Results section, and since the corrections for cross-polarization are small, $\lambda(\sigma/R) = \lambda$(NOE). A 5% accuracy in the "calibration" distance, $r_2 = 2.96$ Å, was assumed. This seems reasonable since $^3J_{\text{NHCH}}$ (val) is large and r_2 is not

TABLE VIII

INTERPROTON DISTANCES CALCULATED FROM RATIOS OF
σ'S AND VICINAL COUPLING CONSTANT DISTANCES

	$^3J_{NHCH}$(phe) = 4.41 Hz	$^3J_{NHCH}$(leu) = 9.94 Hz	$^3J_{NHCH}$(orn) = 10.42 Hz	$^3J_{NHCH}$(val) = 10.22 Hz	Mean	SD
			Å			
r(pro C$^\delta$H1—pro C$^\delta$H2)	1.87	1.94	2.00	1.96	1.93	0.06
	1.88	1.93	1.99	1.95		
		1.92	2.02			
		1.92	2.01			
r(phe C$^\alpha$H—pro C$^\delta$H1)	2.16	2.22	2.30	2.25	2.22	0.07
		2.22				
r(pro C$^\alpha$H—pro C$^\delta$H2)	2.27	2.33	2.41		2.33	0.08
		2.32		2.35		
r(phe NH—phe C$^\alpha$H)	2.84*	2.92	3.02		2.99	0.11
		2.92		2.95		
r(phe NH—leu C$^\alpha$H)	2.19	2.25	2.33	2.28	2.23	0.08
	2.15	2.24	2.35	2.23		
		2.21	2.29			
		2.20				
r(leu NH—leu C$^\alpha$H)	2.86		3.05		2.96	0.11
	2.87	2.95*		2.99		
			3.05	3.02		
r(leu NH—orn C$^\alpha$H)	2.16	2.22	2.30		2.17	0.07
	2.06	2.22	2.32	2.25		
		2.12				
		2.11				
r(orn NH—orn C$^\alpha$H)	2.78	2.86		2.89	2.85	0.10
	2.76	2.85	2.96*			
		2.84				
		2.83				
r(orn NH—val C$^\alpha$H)	2.13	2.19	2.26		2.18	0.07
	2.12	2.18	2.28	2.21		
		2.18	2.25	2.20		
		2.17	(2.28)			
r(val NH—val C$^\alpha$H)	2.84	2.93	3.02	2.96*	2.93	0.10
		2.92	(3.04)			
r(val NH—pro C$^\alpha$H)	2.70	2.77	2.87	2.81	2.78	0.10
		2.77	(2.89)			

*Distances calculated directly from the given, electronegativity-corrected coupling constant by using the Karplus-Bystrov curve and used to calculate the other values in the same column.

a rapidly varying function of ^3J in the region of interest. The accuracies of the other methods are comparable, for example, for r_1 = r(orn NH—val C$^\alpha$H) in Table VII, $\lambda(r_1)$ = 0.13 Å.

In this data set 19 NOE and 8 T_1^{SE} measurements were used to relate, in turn, each of the 5 known, "calibration" distances to the 11 backbone distances calculated. Thus the problem of calculating these distances is overdetermined and the standard devia-

TABLE IX
MEAN VALUES OF INTERPROTON DISTANCES IN GRAMICIDIN S

	Method I (Table VI)	Method II (Table VII)	Method III (Table VIII)	Method IV (Table IX)	Mean	SD
			$\overset{\circ}{A}$			
r(pro C$^\delta$H1—pro C$^\delta$H2)	1.77	2.07	1.77	1.93	1.89	0.14
r(phe C$^\alpha$H—pro C$^\delta$H1)	2.03	2.50	2.04	2.22	2.21	0.21
r(phe C$^\alpha$H—pro C$^\delta$H2)	2.14	2.39	2.14	2.33	2.24	0.14
r(phe NH—phe C$^\alpha$H)	2.57	2.99	2.73	2.99	2.82	0.21
r(phe NH—leu C$^\alpha$H)	1.99	2.31	2.05	2.23	2.15	0.15
r(leu NH—leu C$^\alpha$H)	2.46	2.87	2.71	2.96	2.75	0.22
r(leu NH—orn C$^\alpha$H)	1.86	2.16	2.04	2.17	2.06	0.14
r(orn NH—orn C$^\alpha$H)	2.49	2.90	2.63	2.85	2.72	0.19
r(orn NH—val C$^\alpha$H)	1.90	2.21	2.00	2.18	2.07	0.15
r(val NH—val C$^\alpha$H)	2.55	2.96	2.69	2.93	2.78	0.20
r(val NH—pro C$^\alpha$H)			2.54	2.78	2.66	0.17
					Mean	0.17

[a]-[d]From Tables VI through IX, respectively.

tion (last column, Table IX) of the four separate methods of calculation averages 0.17 Å. These standard deviations are in good agreement with the accuracy, which should be expected based on the full analysis of the propagation of experimental errors.

Summary

The experimental NOE's were corrected for decoupler spillover and cross-polarization to yield σ/R parameters, and the ratios of these parameters for three protons were used to calculate the ratios of interproton distances. A second method of obtaining these interproton distance ratios involved a combination of the NOE between two protons and the value of the selective excitation spin-lattice relaxation time.

To obtain particular interproton distances from interproton distance ratios, two approaches were used; one of the two distances in the ratio was calculated from either (a) geminal group interproton distances (e.g. the pro C$^\delta$H$_2$ group) or (b) distances derived from backbone scalar coupling constants and the appropriate Karplus relationship. All four methods of calculating interproton distances gave a consistent set of backbone interproton distances, the standard deviation from the mean being ±0.17 Å. The methods involving geminal interproton distances always yielded backbone distances 0.1–0.2 Å smaller than those derived by Karplus curve methods. This may indicate some conformational averaging at the pro C$^\delta$H's: additional evaluation of the calibration procedures could lead to further improvements in the accuracy of these methods.

The fact that the distances between the phe^4 alpha proton and the two pro^5 delta protons of gramicidin S are each 2.1 Å is consistent with a β-II$'$ turn for this moiety. The inter- and intraresidue alpha-proton-to-amide-proton distances for the leu^3-phe^4 sequence and the small NOE between the pro^5 alpha and val^1 amide protons also sup-

port this conclusion. The other intra- and interresidue alpha proton-amide proton distances are consistent with gramicidin S having an antiparallel β-pleated sheet, but since one interproton distance defines two ϕ or two ψ angles, other conformations are not rigorously excluded.

REFERENCES

1. KOWALEWSKI, V. J. 1969. The INDOR technique in high resolution nuclear magnetic resonance. Progress in NMR spectroscopy. Vol. 5. J. W. Elmsley, J. Feeney and L. H. Sutcliffe, editors. Pergamon Press, Ltd., Oxford, U.K. 1–31.
2. HOFFMAN, R. A., and S. FORSEN. 1966. High resolution nuclear magnetic double and multiple resonance. Progress in NMR spectroscopy. Pergamon Press, Ltd., Oxford, U.K. Vol. 1. 15–204.
3. GIBBONS, W. A., H. ALMS, J. A. SOGN, and H. R. WYSSBROD. 1972. Homonuclear INDOR as a basis for determining amino acid conformation. *Proc. Natl. Acad Sic. U.S.A.* **69**:1621–1265.
4. GIBBONS, W. A., H. ALMS, R. S. BOCKMAN, and H. R. WYSSBROD. 1972. Homonuclear INDOR spectroscopy as a means of simplifying and analyzing proton magnetic resonance spectra of peptides and as a basis for determining secondary and tertiary conformations of complex peptides. *Biochemistry.* **11**:1721–25.
5. ANET, F. A. L., and A. J. R. BOURNE. 1965. Nuclear magnetic resonance spectral assignments from nuclear Overhauser effects. *J. Am. Chem. Soc.* **87**:5250–5252.
6. GIBBONS, W. A., D. CREPEAUX, J. DELAYRE, J. J. DUNAND, G. HADJUKOVIC, and H. R. WYSSBROD. 1975. The study of peptides by INDOR, difference nmr and time-resolved double resonance techniques. Peptides: Chemistry, Structure and Biology. R. Walter and J. Meienhofer, editors. 127–137.
7. KHALED, M. C., and D. W. URRY. 1976. Nuclear Overhauser enhancement demonstration of type II β-turn peptides of tropoelastin. *Biochem. Biophys. Res. Commun.* **70**:485–491.
8. GLICKSON, J. D., S. L. GORDON, T. P. PITNER, D. G. AGRESTI, and R. WALTERS. 1976. Intramolecular ^{1}H nuclear Overhauser effect study of the solution conformation of valinomycin in dimethyl sulfoxide. *Biochemistry.* **15**:5721–5729.
9. LEACH, S. J. G. NEMETHY, and H. A. SCHERAGA. 1977. Use of proton nuclear Overhauser effects for the determination of conformations of amino acid residues in oligopeptides. *Biochem. Biophys. Res. Commun.* **75**:207–215.
10. RAE, I. D., E. R. STIMSON, and H. A. SCHERAGA. 1977. Nuclear Overhauser effects and the conformation of gramicidin S. *Biochem. Biophys. Res. Commun.* **77**:225–229.
11. BALARAM, P. A., A. A. BOTHNER-BY, and E. BRESLOW. 1973. Nuclear magnetic resonance studies of the interactions of peptides with bovine neuroficin. *Biochemistry.* **12**:4695–4704.
12. FORSEN, S., and R. A. HOFFMAN. 1963. Study of moderately rapid chemical exchange reactions by means of nuclear magnetic double resonance. *J. Chem. Phys.* **39**:2892–2901.
13. PITNER, T. P., J. D. GLICKSON, R. ROWAN, J. DADOK, and A. A. BOTHNER-BY. 1975. Solvation of angiotensin II and gramicidin S determined by NMR solvent saturation methods. *In* Proceedings of the Fourth American Peptide Symposium. Peptides: Chemistry, Structure and Biology. R. Walter and J. Meienhofer, editors. Ann Arbor Science Publishers, Inc., Ann Arbor, Mich. 159–164.
14. SCHWYZER, R., and U. LUDESCHER. 1968. Conformational study of gramicidin S using the phthalimide group as a nuclear magnetic resonance marker. *Biochemistry.* **7**:2519–2522.
15. STERN, A., W. A. GIBBONS, and L. C. CRAIG. 1968. A conformational analysis of gramicidin S by nuclear magnetic resonance. *Proc. Natl. Acad. Sci. U.S.A.* **61**:734–41.
16. SCHWYZER, R., and U. LUDESCHER. 1969. Investigations of the cyclic hexapeptide cyclo(glyprogly)$_2$

by means of proton magnetic resonance and parallel studies on the cyclodecapeptide gramicidin S. *Helv. Chim. Acta.* **52**:2033-2040.

17. FINER, E. G., H. HAUSER, and D. CHAPMAN. 1969. Nuclear magnetic resonance studies of interactions of phospholipids with cyclic antibiotics. *Chem. Phys. Lipids.* **3**:386-392.

18. OVCHINNIKOV, Y. A., U. T. IVANOV, V. F. BRYSTROV, A. I. MIROSHNIKOV, E. N. SHEPEL, N. A. ABDULLAEV, E. S. EFREMOV, and N. B. SENYAVINA. 1970. The conformation of gramicidin S and its N,N′-diacetyl-derivative in solution. *Biochem. Biophys. Res. Commun.* **39**:217-225.

19. SUGANO, H., H. ABE, M. MIYOSHI, T. KATO, and N. IZUMIYA. 1973. Gramicidin S analogs containing N-methylleucine in place of leucine. *Experientia (Basel).* **29**:1488-89.

20. SOGN, J. A., L. C. CRAIG, and W. A. GIBBONS. 1974. The complete assignments of the ^{13}C magnetic resonance spectrum of gramicidin S by biosynthetic enrichment studies. *J. Am. Chem. Soc.* **96**: 3306-3309.

21. ALLERHAND, A., and R. A. Komorski. 1973. Study of internal rotations in gramicidin S by means of carbon-13 spin-lattice relaxation measurements. *J. Am. Chem. Soc.* **95**:8828-8831.

22. PITNER, T. P., and D. W. URRY. 1972. Proton magnetic resonance studies in trifluoroethanol: solvent-mixtures as a means of delineating peptide protons. *J. Am. Chem. Soc.* **94**:1399-400.

23. ZHUZE, A. L., G. A. KROGAN, N. A. KRIT, T. M. ANDRONOVA, M. P. FILATOVA, L. B. SENYAVINA, E. A. MESHCHERYAKOVA, I. D. RYABOVA, G. A. RAVDEL, and L. A. SHCHUKINA. 1974. Depsipeptide modification as a method of determining the contribution of intramolecular hydrogen bonds to conformational stability of peptides (gramicidin S). *Med. Biol. Eng.* **8**:69-74.

24. KOMORSKI, R. A., I. R. PEAT and G. C. LEVY (1975). High field carbon-13 NMR spectroscopy: Conformational mobility in gramicidin S and frequency dependence of carbon-13 spin-lattice relaxation times. *Biochem. Biophys. Res. Commun.* **65**:272-279.

25. KUMAR, N. G., N. IZUMIYA, M. MIYOSHA, H. SUGANO, and D. W. URRY. 1975. Conformational and spectral analysis of the polypeptide antibiotic N-methylleucine gramicidin S hydrochloride by nuclear magnetic resonance. *Biochemistry.* **14**:2197-2207.

26. HAWKES, G. E., E. W. RANDALL, and C. H. BRADLEY. 1975. Theory and practice for studies of peptides by N-15 nuclear magnetic resonance at natural abundance: gramicidin S. *Nature (Lond.).* **257**: 767-772.

27. URRY, D. W., M. M. LONG, L. W. MITCHELL, and K. OKAMOTO. 1975. Utilization of proton and ^{13}C magnetic resonance in the evaluation of polypeptide secondary structure in solution. *In* Proceedings of the Fourth American Peptide Symposium. Peptides Chemistry, Structure and Biology. R. Walter and J. Meienhofer, editors. Ann Arbor Science Publishers, Inc., Ann Arbor, Mich.

28. PATEL, D. J., and A. E. TONELLI. 1976. N-Methylleucine gramicidin S and (di-N-methylleucine) gramicidin S conformation with cis-L-orn-L-N-methylleucine bonds. *Biopolymers.* **15**:1623-35.

29. DYGERT, M., N. GO, and H. A. SCHERAGA. 1975. Use of a symmetry condition to compute the conformation of gramicidin S. *Macromolecules.* **8**:750-761.

30. BAYLEY, P. M. 1971. The conformation of gramicidin S: computed circular dichroism properties. *Biochem. J.* **125**:908-71P.

31. MOMANY, F. A., C. VANDERKOOI, R. W. TUTTLE, and H. A. SCHERAGA. 1969. Minimization of polypeptide energy IV. Further studies of gramicidin S. *Biochemistry.* **8**:744-46.

32. PYSH, E. 1970. Conformations at local energy minima for gramicidin S: optical calculations. *Science (Wash. D.C.).* **167**:290-292.

33. SCHERAGA, H. A. 1969. Calculations of polypeptide conformations. *Harvey Lect.* **63**:99-138.

34. DE SANTIS, P., and A. M. LIQUORI. 1971. Conformation of gramicidin S. *Biopolymers.* **10**:699-710.

35. JONES, C. R., J. B. ALPER, M. KUO, and W. A. GIBBONS. 1977. Multiple conformations of the zwitterionic and cationic forms of enkephalins and other peptides. Peptides: Proceedings of the Fifth American Peptide Symposium, M. Goodman and J. Meienhofer, editors. J. Wiley & Sons, Inc., New York. 329-332.

36. KUO, M., C. R. JONES, and W. A. GIBBONS. 1978. Multiple solution conformations and internal rotations of the decapeptide gramicidin S. *J. Biol. Chem.* In press.

37. KUO, M., C. R. JONES, T. H. MAHN, P. R. MILLER, L. J. F. NICHOLLS, and W. A. GIBBONS. 1978. Simplification and spin-spin analysis of the side-chain proton magnetic resonance spectrum of the decapeptide gramicidin S using difference scalar decoupling and biosynthesis of selectively deuterated analogs. *J. Biol. Chem.* In press.

38. NOGGLE, J. H., and R. E. SCHIRMER. 1971. The Nuclear Overhauser Effect. Academic Press, Inc., New York. Chapter 3. pp 44–76.

39. FREEMAN, R., H. D. W. HILL, B. L. TOMLINSON, and L. D. HALL. 1974. Dipolar contribution to NMR spin-lattice relaxation of protons. *J. Chem. Phys.* **61**:4466–4473.

40. BOCK, K., and L. D. HALL. 1977. Conformational studies of nucleosides by measurements of proton spin lattice rates. *J. Carbohydr. Nucleosides Nucleotides.* **4**:83–92.

41. MOMANY, F. A., R. F. McGUIRE, A. W. BURGESS, and H. A. SCHERAGA. 1975. Energy parameters in polypeptides. VII. Geometric parameters, partial atomic charges, nonbonded interactions, hydrogen bond interactions, and intrinsic torsional potentials for the naturally occurring amino acids. *J. Phys. Chem.* **79**:2361–2381.

42. BYSTROV, V. F. 1976. Spin-spin coupling and the conformational states of peptide systems. *Prog. NMR Spectroscopy.* **10**:41–81.